

# Vibrational Feshbach resonances in electron attachment to carbon dioxide clusters<sup>\*</sup>

 E. Leber, S. Barsotti, I.I. Fabrikant<sup>a</sup>, J.M. Weber<sup>b</sup>, M.-W. Ruf, and H. Hotop<sup>c</sup>

Fachbereich Physik, Universität Kaiserslautern, 67663 Kaiserslautern, Germany

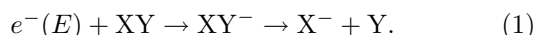
Received 11 January 2000 and Received in final form 10 April 2000

**Abstract.** Using a high resolution ( $\Delta E \approx 1$  meV) laser photoelectron attachment method, we have studied the formation of  $(\text{CO}_2)_q^-$  ions ( $q = 4\text{--}22$ ) in collisions of low energy electrons (1–180 meV) with  $(\text{CO}_2)_N$  ( $q \leq N$ ) clusters. The previously reported “zero energy resonance”, observed at much larger electron bandwidths, actually consists of several narrow vibrational Feshbach resonances of the type  $[(\text{CO}_2)_{N-1}\text{CO}_2(\nu_i)]^-$  which involve a vibrationally-excited molecular constituent ( $\nu_i \geq 1$  denotes vibrational mode) and a diffuse electron weakly bound to the cluster by long range forces. The resonances occur at energies below those of the vibrational excitation energies of the neutral clusters  $[(\text{CO}_2)_{N-1}\text{CO}_2(\nu_i)]$ ; the redshift rises with increasing cluster ion size  $q$  by about 12 meV per unit; these findings are recovered by a simple model calculation for the size dependent binding energies. The size distribution in the cluster anion mass spectrum, resulting from attachment of very slow electrons, mainly reflects the amount of overlap of solvation-shifted vibrational resonances with zero energy; the cluster anion size  $q$  is identical with or close to that of the attaching neutral cluster.

**PACS.** 34.80.Ht Dissociation and dissociative attachment by electron impact – 36.40.Wa Charged clusters – 34.80.Gs Molecular excitation and ionization by electron impact

## 1 Introduction

It is well-known that temporary negative ion states  $\text{XY}^-$ , formed in low energy electron collisions with molecules  $\text{XY}$ , are crucial for vibrational excitation as well as for formation of anions  $\text{X}^-$  through dissociative attachment (DA) [1–7]:



Both shape resonances (electrons trapped within a centrifugal barrier) and Feshbach resonances (electrons attached to electronically excited states  $\text{XY}^*$  of the neutral molecule) are representatives of such temporary negative ion states in which the incoming electron is captured for a time interval long compared to the collision time and often similar to or even larger than a typical vibrational period. In special cases, such as molecules with a sufficiently strong permanent dipole moment, resonances attached to vibrationally excited levels of the electronic

ground state (here addressed as vibrational Feshbach resonances VFR) may occur [8–10]. Recently, a clear VFR has been detected in a joint experimental and theoretical study of dissociative attachment (DA) to methyl iodide ( $\text{CH}_3\text{I}$ ) [11] yielding  $\text{I}^-$ : below the onset for excitation of the symmetric stretch C–I vibration ( $\nu_3 = 1$ ), a prominent peak is observed (width about 10 meV), followed by a cusp at threshold. Subsequent DA experiments involving methyl iodide clusters revealed a strong influence of the cluster environment: for the smallest cluster ion  $\text{CH}_3\text{I}\cdot\text{I}^-$  the clear VFR present in DA to the monomer was found to change into a weak, broad shoulder shifted to lower energy [12]. Very recently, astoundingly narrow resonances (width few meV) were observed in electron attachment collisions with  $(\text{N}_2\text{O})_N$  clusters (yielding  $(\text{N}_2\text{O})_q\text{O}^-$  ions ( $q < N$ )) and interpreted as vibrational Feshbach resonances of the type  $[(\text{N}_2\text{O})_{N-1}\text{N}_2\text{O}(\nu_i)]^-$  which involve a vibrationally-excited molecular constituent ( $\nu_i \geq 1$  denotes vibrational mode) and a diffuse, weakly-bound electron [13]. The resonances were found to be located at energies slightly below those of the  $\nu_i$  excitation energy of the neutral clusters  $[(\text{N}_2\text{O})_{N-1}\text{N}_2\text{O}(\nu_i)]$  with redshifts rising weakly with increasing cluster ion size  $q = 5\text{--}8$ . Previous low resolution work on negative cluster ion formation from  $\text{N}_2\text{O}$  clusters [14–17] as well as clusters of other molecules with negative electron affinities, *e.g.*  $\text{CO}_2$  [14–18], had shown a resolution-limited “zero energy resonance” (width about 0.5 eV) whose influence increased with cluster size,

<sup>\*</sup> Work based in part on the unpublished doctoral dissertation of E. Leber (Fachbereich Physik, Universität Kaiserslautern, December 1999).

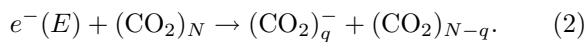
<sup>a</sup> *Permanent address:* Department of Physics and Astronomy, University of Nebraska, Lincoln, NE 68588-0111, USA.

<sup>b</sup> *Present address:* Sterling Chemistry Laboratory, Yale University, P.O. Box 208107, New Haven, CT 06520-8107, USA.

<sup>c</sup> e-mail: hotop@physik.uni-kl.de

but the nature of this intriguing phenomenon had remained uncertain. To investigate the possible generality of the occurrence of VFRs in DA to molecular clusters we extended our studies to clusters of carbon dioxide ( $\text{CO}_2$ ).

Pioneering work on anion formation in energy-controlled electron collisions with  $\text{CO}_2$  clusters was carried out by Klots and Compton [14], by Knapp *et al.* [15–17], and by Stamatovic *et al.* [18, 19]. The well-known DA resonance for the  $\text{CO}_2$  molecule, located at 4.4 eV [20] and yielding  $\text{O}^-$  ions, is also active in heterogeneous  $(\text{CO}_2)_q\text{O}^-$  ( $q \geq 1$ ) and homogeneous  $(\text{CO}_2)_q^-$  ( $q \geq 2$ ) cluster anion formation, but appears shifted to lower energies with increasing cluster size [14, 16, 17, 19]. The mass spectrum of homogeneous  $(\text{CO}_2)_q^-$  ions exhibited maxima at  $q = 10, 14,$  and  $16$  (most clearly at low electron energies) [15, 19]. Similar mass spectra were observed by Alexander *et al.* [21] as well as Haberland *et al.* [22] with electrons of undefined energy mixed into the condensation zone of a supersonic expansion and by Kondow *et al.* [23, 24] as well as Kraft *et al.* [25] in Rydberg electron transfer (RET). Studies of the  $(\text{CO}_2)_q^-$  ion intensities as a function of stagnation pressure by Stamatovic *et al.* revealed similar growth curves for  $(\text{CO}_2)_3^-$  ions produced at an electron energy of about 3 eV and for  $(\text{CO}_2)_9^-$  ions, formed with electrons of near-zero energy. This result was interpreted to indicate [19] that only little or no evaporation of  $\text{CO}_2$  molecules occurs in attachment at very low electron energies (the excess energy being distributed among the large number of degrees of freedom) while at  $E = 3$  eV several molecules leave the cluster following electron capture:



In contrast, Kondow *et al.* [23, 24] interpreted their  $(\text{CO}_2)_q^-$  mass spectrum due to RET from (unselected)  $\text{Kr}^{**}$  Rydberg atoms (principal quantum numbers around 25) somewhat differently: from the width of the region of weak cluster ion intensities ( $q = 11$ – $13$ ) the average number ( $N - q$ ) of  $\text{CO}_2$  molecules, evaporated in the stabilization process, was estimated to be at least 4, and from the smallest cluster ion detected ( $q = 3$ ), the threshold size for the primary electron attachment process was estimated to be at least  $N_L = 7$ , in agreement with a theoretical model promoted by Tsukada *et al.* [26]. These authors developed a theory for electron attachment to van der Waals clusters and applied it to  $\text{CO}_2$  clusters. According to their model, initial attachment proceeds to “extended affinity” (*i.e.* delocalized) states, from which quick stabilization occurs to a state where the electron is localized on a few molecular centers (cluster ion core). The released stabilization energy is transferred to inter- and intramolecular vibrational modes (“phonon modes”), corresponding to heating of the cluster and inducing evaporation processes which lead to intensity anomalies related to cluster-ion stability. Tsukada *et al.* found that the (primary) attachment cross-section is negligibly small for  $N < 7$  (“threshold size”  $N_L = 7$ ) and that the attachment cross-sections decrease sharply from zero with rising electron energy (no

analytical expression for the threshold energy dependence was given). Information on the size of the cluster ion core has been provided by photoelectron spectroscopy of stabilized  $(\text{CO}_2)_q^-$  ions ( $q = 2$ – $16$ ) [27, 28]: the  $(\text{CO}_2)_2^-$  dimer ion forms the cluster core for  $q = 2$ – $5$  and for  $q = 14$ – $16$  while the  $\text{CO}_2^-$  ion is the cluster kernel for  $q = 7$ – $13$  (for  $(\text{CO}_2)_6^-$  both the monomer and the dimer ion coexist as cores).

These partly contradictory findings and claims warrant more direct experimental evidence in order to clarify the nature of the “zero energy resonance” and the mechanism of cluster ion formation at low electron energies. Weber *et al.* [29] have recently shown in a high resolution experiment ( $\Delta E \approx 1$  meV) involving small water clusters that non-evaporative ( $q = N$ ) attachment yielding long-lived cluster ions with  $q = 2, 6, 7$  does in fact occur in free electron capture collisions at a few meV energy. In the present paper, we demonstrate that  $(\text{CO}_2)_q^-$  ion formation ( $q = 4$ – $22$ ) from  $(\text{CO}_2)_N$  ( $q \leq N$ ) clusters largely proceeds through vibrational Feshbach resonances of the type observed for electron attachment to  $\text{N}_2\text{O}$  clusters. For  $\text{CO}_2$  clusters, however, the widths and the redshifts are substantially larger than for  $\text{N}_2\text{O}$  clusters, thereby allowing clear statements on the relation between the size  $N$  of the neutral cluster and the resulting cluster ion size  $q$  and on the origin of substantial changes in the shape of the  $(\text{CO}_2)_q^-$  anion mass spectra at near zero electron energies.

## 2 Experimental

Our experiment is based on the Laser Photoelectron Attachment (LPA) method introduced by Klar *et al.* [30, 31]: energy-variable, monoenergetic electrons are created by photoionization of atoms in a collimated beam; they interact with the target molecules (clusters) of interest in the region where the photoionization process takes place. While in our previous LPA investigations, photoionization of laser-excited  $\text{Ar}^*(4p, J = 3)$  atoms yielded electron currents up to 1 pA, we have now used an analogous scheme with a demonstrated potential for nA currents, namely photoionization of laser-excited  $\text{K}^*(4p_{3/2})$  atoms [13, 29]. Both hyperfine components of ground state  $^{39}\text{K}(4s, F = 1, 2)$  atoms in a collimated beam of potassium atoms (collimation 1:400, diameter 1.5 mm) from a doubly differentially pumped metal vapour oven are transversely excited to the  $^{39}\text{K}^*(4p_{3/2}, F = 2, 3)$  states by the first sidebands of the electro-optically modulated (frequency 220.35 MHz) output of a single mode CW titanium: sapphire laser ( $\lambda_1 = 766.7$  nm). Part of the excited state population is transferred to high Rydberg levels ( $nd, (n + 2)s, n \geq 12$ ) or photoionized by interaction with the intracavity field of a broadband (40 GHz) tunable dye laser (power up to 5 W), operated in the blue spectral region ( $\lambda_2 = 472$ – $424$  nm, dye Stilbene 3). The energy of the photoelectrons can be continuously varied over the range 0–200 meV by tuning the wavelength of the ionizing laser ( $\lambda_2 < 455$  nm).

Electrons, created in the overlap volume of the potassium atom beam and the laser beams, may attach to molecules and clusters in a collimated, differentially pumped nozzle beam (diameter in the reaction region 3 mm; nozzle diameter  $d_0 = 60 \mu\text{m}$ , stagnation pressures  $p_0$  up to 5 bar, nozzle temperature  $T_0 = 300 \text{ K}$ ), propagating in a direction perpendicular to both the potassium and the laser beams. Anions, generated by electron attachment and drifting out of the essentially field free reaction chamber, are imaged into a quadrupole mass spectrometer ( $m/q \leq 2000 \text{ u/e}$ ) and detected by a differentially pumped off axis channel electron multiplier. For the sake of normalization and resolution testing, using the well-known cross-section for  $\text{SF}_6^-$  formation from  $\text{SF}_6$ , the target gas mixture (50%  $\text{CO}_2$  seeded in He) contains 0.15% of  $\text{SF}_6$  molecules. The reaction volume is surrounded by a cubic chamber made of oxygen free, high conductivity copper, the inner walls of which are coated with colloidal graphite. By applying bias potentials to each face of the cube, DC stray electric fields are reduced to values  $F_S \leq 70 \text{ mV/m}$ . Magnetic fields are reduced to values below  $2 \mu\text{T}$  by compensation coils located outside the vacuum apparatus. The electron energy resolution is limited by the bandwidth of the ionizing laser ( $\Delta E_L \approx 150 \mu\text{eV}$ ), residual electric fields ( $\Delta E_F \leq 105 \mu\text{eV}$ ), the Doppler effect caused by the target velocity ( $\Delta E_D \approx 0.07\sqrt{E}$ ,  $\Delta E_D$  and electron energy  $E$  in meV), and space charge effects due to  $\text{K}^+$  photoions generated in the reaction volume (depending on the  $\text{K}^+$  current). An upper limit to the overall energy spread close to  $E = 0 \text{ eV}$  can be estimated by comparison of the  $\text{SF}_6^-$  ion yield, measured under the same conditions as the cluster ion yield, with the cross-section measured by Klar *et al.* [30] at sub-meV resolution and is determined to be  $\Delta E_{\text{max}} \approx 1.2 \text{ meV}$  in the present experiment (electron current around 20 pA).

### 3 Results and discussion

Only homogeneous ions  $(\text{CO}_2)_q^-$  ( $q \geq 4$ ) were observed in the negative ion mass spectra, both in Rydberg electron transfer (RET) for principal quantum numbers  $n = 12\text{--}300$  and in free electron attachment for the energy range  $E = 1\text{--}200 \text{ meV}$ . In Figure 1 we show the  $(\text{CO}_2)_q^-$  cluster anion size distribution ( $q = 4\text{--}24$ ), observed for RET at  $n = 30$  (a) and  $n \approx 300$  (b), *i.e.* for electron collisions at practically zero energy [32, 33]. The results for  $n = 30$  are in good agreement with those reported by Kraft *et al.* [25] (at  $q > 17$ , the intensities in the present spectrum are smaller than those of Kraft *et al.* [25] which we attribute to differences in the neutral cluster size distribution); this mass spectrum shows maxima at  $q = (9, 10), 14$ , and 16, as observed before in RET with a broad  $n$  distribution by Kondow *et al.* [23, 24] and in free electron attachment at low energies [15, 19, 21, 22]. We note that both anion cluster size distributions shown in Figure 1 are completely different from the expected size distribution of neutral clusters (slow decrease towards larger  $N$ , see also [25]). The spectrum in Figure 1b, which

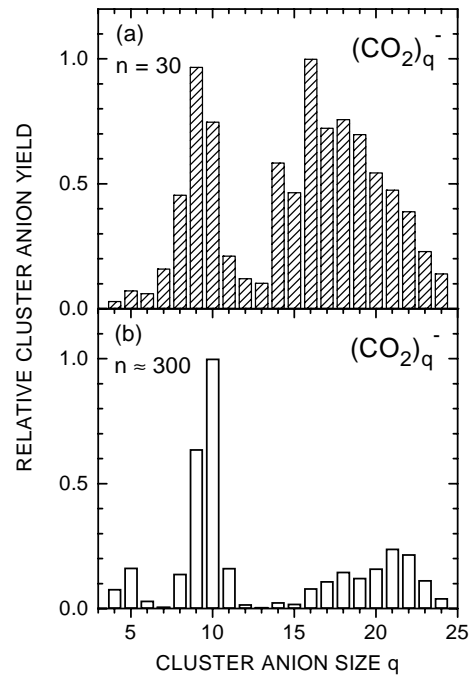


**Fig. 1.** Anion cluster size distributions ( $(\text{CO}_2)_q^-$ ,  $q = 4\text{--}24$ ), as measured for Rydberg electron transfer (RET) to neutral carbon dioxide clusters ( $(\text{CO}_2)_N$ ,  $N \geq q$ ); (a): Rydberg electron principal quantum number  $n = 30$  (binding energy  $E_n = 15 \text{ meV}$ , *i.e.* effective collision energy  $E \approx 3 \text{ meV}$  [32]), (b):  $n \approx 300$  ( $E_n \approx 0.15 \text{ meV}$ , *i.e.*  $E \approx 0 \text{ meV}$ ).

represents a genuine threshold electron attachment mass spectrum ( $n \approx 300$ ,  $E \approx 0 \text{ meV}$ ), is reported for the first time. In view of the rather small change in effective electron energy from  $n = 30$  ( $E \approx 3 \text{ meV}$  [32]), the spectrum in Figure 1b is quite different from that in Figure 1a. The minima around  $q = 7$  and  $q = 13$  are now very deep, indeed; the maximum at  $q = 10$  stands out clearly whereas maxima at  $q = 14$  and 16 are no longer observed. The free electron attachment spectra, studied for  $q = 4\text{--}22$ , will provide insight to understand the shape of the anion size distributions in Figure 1.

In Figure 2 we present the energy dependent yield for  $(\text{CO}_2)_q^-$  ( $q = 5\text{--}12$ ) ions over the energy range from 1 meV up to 180 meV, using an intensity scale common to all  $q$ . Two clearly separated series of resonances are observed which exhibit redshifts increasing by about 12 meV per monomer unit. The key spectrum observed for  $q = 5$  shows a distinct zero energy peak (indicative of  $s$ -wave attachment), a rather sharp resonance peaking at about 52 meV and a double-peak structure with a center-of-gravity around 134 meV. We interpret these three peaks to be associated with vibrationally excited temporary negative cluster ion states (vibrational Feshbach resonances VFRs) of the type  $[(\text{CO}_2)_{N-1}\text{CO}_2(\nu_i)]^-$  with  $(\nu_1 \nu_2 \nu_3) = (010)$  and  $(020)/(100)$ , respectively, which evolve into the observed long-lived  $(\text{CO}_2)_{q=5}^-$  anions either by redistribution of the vibrational energy among soft modes of the cluster with formation of a metastable cluster ion with  $q = N$  or by evaporation of a small number of  $\text{CO}_2$  units

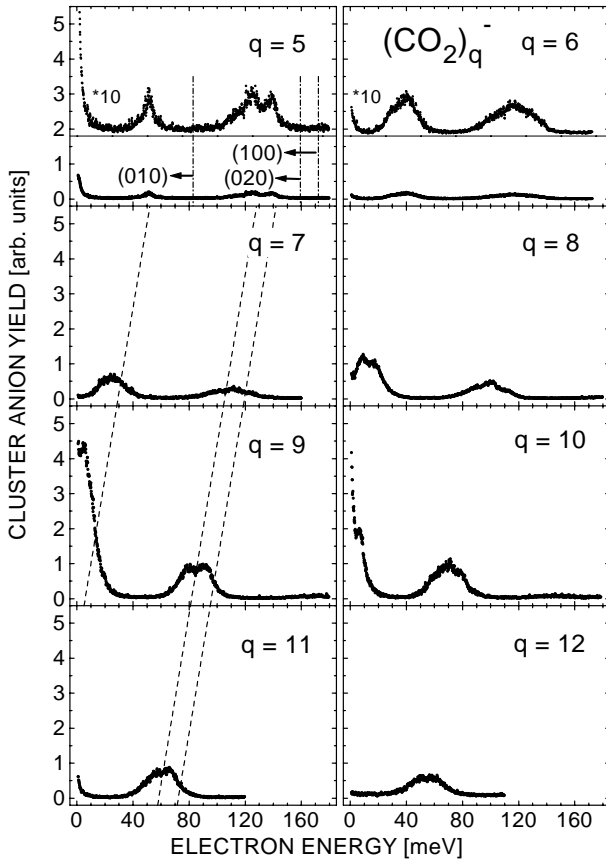


**Fig. 2.** Ion yields for the formation of homogeneous  $(\text{CO}_2)_q^-$  anions ( $q = 5-12$ ) in free electron attachment to neutral carbon dioxide clusters ( $(\text{CO}_2)_N$ ,  $N \geq q$ ). The spectra have a common intensity scale. For  $q = 5$ , the energy positions of the  $(\nu_1\nu_2\nu_3) = (010)$ ,  $(020)$  and  $(100)$  vibrational modes in the  $\text{CO}_2$  monomer are indicated by vertical dash-dotted lines. For  $q = 5, 7, 9$  and  $11$ , the respective positions of vibrational Feshbach resonances are connected by dashed lines, illustrating a redshift of about 12 meV per monomer unit.

(most likely  $N - q = 1$ , see below). As expected for VFRs their respective energies are redshifted from those of the neutral  $[(\text{CO}_2)_{N-1}\text{CO}_2(\nu_i)]_N$  precursor. In contrast to the case of  $\text{N}_2\text{O}$  clusters, however, the redshift is substantially larger for  $\text{CO}_2$  clusters indicating a stronger interaction of the resonantly-captured electron with  $\text{CO}_2$  clusters than with  $\text{N}_2\text{O}$  clusters. In line with this observation the resonance widths are larger for  $\text{CO}_2$  clusters than for  $\text{N}_2\text{O}$  clusters. For any particular  $(\text{CO}_2)_q^-$  cluster ion, the width of the observed resonances contains contributions due to the intrinsic resonance widths and resonance positions of all involved neutral precursors which participate in VFR formation, *i.e.* the observed resonances are in general inhomogeneously broadened. In view of the substantial redshift of about 12 meV per added  $\text{CO}_2$  unit and the comparatively narrow intrinsic width of the VFRs, the width in conjunction with the redshift of the VFR allows rather direct conclusions to be drawn on the size range of the involved neutral precursors. For  $q = 5$  the resonances exhibit the smallest widths and it is plausible that the attachment

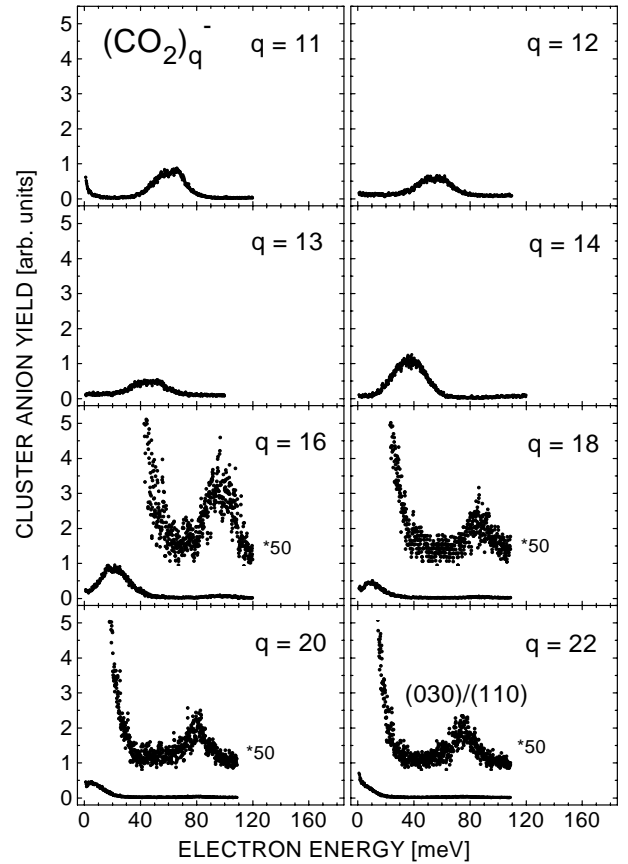


**Fig. 3.** Ion yields for the formation of homogeneous  $(\text{CO}_2)_q^-$  anions ( $q = 11-14, 16, 18, 20, 22$ ) in free electron attachment to neutral carbon dioxide clusters ( $(\text{CO}_2)_N$ ,  $N \geq q$ ). The spectra have a common intensity scale. For  $q \geq 16$ , additional vibrational Feshbach resonances, attributed to the  $(030)$  and  $(110)$  vibrational modes of  $\text{CO}_2$ , are clearly observed.

spectrum is predominately associated with a single neutral precursor size (with the possibility of inhomogeneous broadening due to contributions from different conformations for that cluster size). For  $q \geq 6$ , the  $(010)$  resonances appear to be significantly broader than for  $q = 5$ ; this may indicate contributions from two neighbouring neutral precursor sizes, but could also be caused (at least in part) by the influence of different conformations for a particular  $N$ . In Figure 3 we show the attachment spectra for  $(\text{CO}_2)_q^-$  anion formation for the cluster sizes  $q = 11-22$ . The trends are similar to those observed in Figure 2; the redshifts per added molecular unit decrease somewhat at higher  $q$ . In the attachment spectra for  $q = 16, 18, 20, 22$  vibrational resonances which we attribute to the bending overtone  $(030)$  and the combination vibration  $(110)$  are weakly, but clearly observed.

In Figure 4 we summarize the resonance positions  $E_R$  of all experimentally observed vibrational Feshbach resonances (including those for  $q = 4$  not shown in Figs. 2 and 3). The positions labelled by full symbols correspond to the respective center-of-gravity for the  $(010)$  sequence (circles), the average of the two  $(020)$  and  $(100)$  series (squares), and the average of the two  $(030)$  and

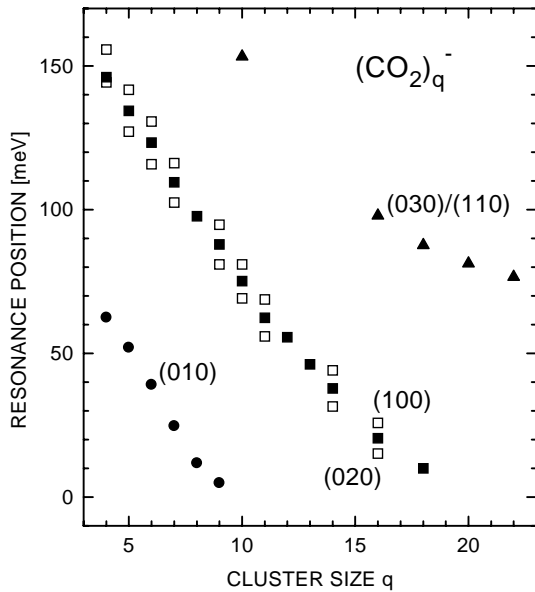


**Fig. 4.** Center-of-gravity energy positions of experimentally observed vibrational Feshbach resonances; full circles:  $(\nu_1\nu_2\nu_3) = (010)$  series, full squares: average of the two (020) and (100) series (the individual positions of which are indicated by open squares), full triangles: average of the two (030) and (110) series (see text).

(110) series (triangles). For each vibrational series, the resonance position  $E_R$  of the VFR mirrors the binding energy  $E_B$  ( $E_B < 0$ , *i.e.* redshift) of the captured electron in the  $[(\text{CO}_2)_{N-1}\text{CO}_2(\nu_i)]^-$  anion state relative to the energy  $E_N$  of the neutral  $[(\text{CO}_2)_{N-1}\text{CO}_2(\nu_i)]$  cluster which carries the same quanta of intramolecular vibrational energy ( $E_R = E_N + E_B$ ). If the geometric arrangement of the cluster constituents does not change upon capture of the electron, the binding energy  $E_B$  can be estimated with a simple calculation, based on the long-range attraction between the electron and the cluster, including an appropriate short range interaction  $U_0$  at distances smaller than the cluster radius  $R_N$ . We only take into account the polarization attraction  $V_{\text{pol}} = -Ne^2\alpha(\text{CO}_2)/2r^4$  (assuming that the effects associated with the quadrupole moment of the  $\text{CO}_2$  molecules can be neglected in the average over the cluster) and cut it off at the cluster radius; moreover, we set  $U_0$  constant at electron-cluster distances smaller than  $R_N = R_0(1.5N)^{1/3}$  ( $R_0 = \text{effective radius of a monomer}$ ) and treat  $U_0$  as a parameter. Figure 5 shows the results of these calculations for the electron binding energies to clusters with  $N = 4-22$ , using six constant values of short range potentials  $U_0$ , the isotropic monomer polarizability  $\alpha(\text{CO}_2) = 20a_0^3$  [34] and  $R_0 = 3 a_0$  ( $a_0 = 52.9 \text{ pm}$ ).

For comparison with the calculated binding energies (lines), the experimentally derived binding energies  $E_B$ , calculated from the resonance positions  $E_R$  (Fig. 4) through  $E_B = E_R - E_N$  are included in Figure 5. In view of the fact that the intramolecular excitation energies  $E_N$  in  $\text{CO}_2$  clusters deviate from those in the  $\text{CO}_2$  monomer  $E_1$  by no more than about  $\pm 1 \text{ meV}$  [35–40]

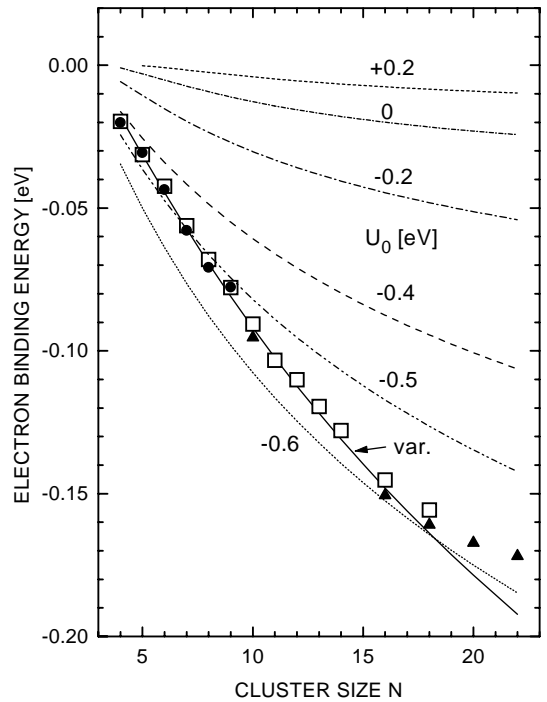


**Fig. 5.** Model calculation of electron binding energies to  $(\text{CO}_2)_N$  clusters ( $N = 4-22$ ) for different short range interactions  $U_0$  in comparison with experimental data (assuming  $q = N$ ); full circles:  $(\nu_1\nu_2\nu_3) = (010)$  series, open squares: average of the two (020) and (100) series, full triangles: average of the two (030) and (110) series (for details see text).

we approximate  $E_N$  by  $E_1$  for all sizes  $N$  of interest:  $E_{(010)} = 82.7 \text{ meV}$ ,  $E_{(020)/(100)} = 165.7 \text{ meV}$ , and  $E_{(030)/(110)} = 248.5 \text{ meV}$  [41], using the average energies for (020)/(100) and (030)/(110), respectively. One observes reasonable agreement between the thus calculated and the observed resonance positions for  $U_0 = -0.5 \text{ eV}$ , if one assumes  $q = N$  (although we do not take this agreement as a proof that  $q = N$ , the comparison indicates that it is reasonable to assume that  $q$  is close to  $N$ ). The calculated average radius of the electron in these resonance states is quite large (about  $20a_0$  for cluster sizes  $N$  around 12) and only weakly dependent on  $N$ . Our model is consistent with the theory of electron affinity of clusters [42], however it does not take into account the variation of the depth of the potential inside the cluster with the cluster size. *Ab initio* calculations discussed in [42] show that this dependence can be approximated by

$$U_0 = aN^{-1/3} + b. \quad (3)$$

The curve “var” in Figure 5 represents the results for the binding energy obtained by using (3) with  $a = 0.7 \text{ eV}$  and  $b = -0.866 \text{ eV}$ . We see that the inclusion of the variable depth leads to a faster variation of the binding energy with  $N$  and improves agreement with the experiment.

We note that the results of the model calculation with  $U_0 = 0.2 \text{ eV}$  (Fig. 5) are in qualitative agreement with the observations of small redshifts for the VFRs in  $\text{N}_2\text{O}$

clusters. This may be taken as indication that the aforementioned difference between the VFRs in CO<sub>2</sub> and N<sub>2</sub>O clusters (larger redshift for CO<sub>2</sub>) lies in the average short range interaction between the electron and the respective molecular constituents (the polarizabilities of N<sub>2</sub>O and CO<sub>2</sub> agree to within 5% [34]). This conclusion is confirmed by analysis of experimental results and theoretical calculations of low-energy electron scattering by CO<sub>2</sub> and N<sub>2</sub>O molecules. Cross-sections for low-energy electron scattering by CO<sub>2</sub> are rapidly increasing towards lower energies [43–45] approaching 200 Å<sup>2</sup> which corresponds to a large negative scattering length of about  $-7.5a_0$ . More recent experimental data [46] on  $e^-$ -CO<sub>2</sub> scattering confirm earlier swarm results [43], but do not cover the low-energy region important for our discussion. Two recent calculations [47, 48] also do not give enough details about the cross-section behaviour below 0.1 eV. Moreover, it seems that both calculations strongly underestimate the cross-sections in the low-energy region because of the low effective polarizability. In particular, excited configurations included in calculations in [48] account only for 10% of the long range polarizability. To show the importance of the polarization interaction in low-energy electron scattering by nonpolar molecules, we write down the first two terms of the modified effective range expansion [49] for the elastic scattering cross-section  $\sigma$

$$\sigma = 4\pi(A^2 + (4/45)Q^2 + Bk + \dots) \quad (4)$$

where  $k = (2E)^{1/2}$ ,  $A$  is the scattering length,  $Q$  is the quadrupole moment, and  $B$  is a coefficient which depends on  $A$ ,  $Q$ , and the isotropic and anisotropic polarizabilities  $\alpha_0$  and  $\alpha_2$ , respectively. The term linear in  $k$  controls the low-energy behavior of the cross-section. In particular, the Ramsauer-Townsend minimum exists if  $B < 0$ . The quadrupole moment contribution to  $B$  is less than 10% for CO<sub>2</sub> [49], and the second term in (4) can be considered as a renormalization of the scattering length. Therefore our model for clusters (short-range well plus polarization tail) can also describe electron scattering by monomers. Indeed, the discussed results [43–45] on low-energy  $e^-$ -CO<sub>2</sub> scattering can be reproduced by including the short-range interaction in the form of an attractive potential well with a depth of about 0.1 eV, although it should be emphasized that a more realistic pseudopotential for the  $e^-$ -CO<sub>2</sub> interaction should include a strong repulsive part [50] which takes into account the Pauli exclusion principle.

On the other hand, experimental [51] and theoretical [52, 53] data on electron scattering by the N<sub>2</sub>O molecule show that the low-energy cross-section in this case is much smaller and does not exceed 8 Å<sup>2</sup> below  $E = 1$  eV. At ultralow energies, the cross-section should increase due to the (albeit very small,  $\mu = 0.16$  D [34]) dipole moment, but this effect should not be important for clusters. The observed behavior can be reproduced by modelling the  $e^-$ -N<sub>2</sub>O interaction potential as a repulsive barrier with a polarization tail which is consistent with our findings for N<sub>2</sub>O clusters.

The attachment spectra shown in Figures 2 and 3 offer the following explanation for the strongly  $q$ -dependent ion intensities in the mass spectrum resulting from threshold electron attachment (Fig. 1b) with a clear maximum at  $q = 10$  and another broad maximum for  $q$  around 21. Enhanced cluster ion intensities are found for  $q$ -values for which a substantial overlap of a VFR with zero electron energy exists. For  $q = 9, 10$ , the (010) resonance has moved close to zero energy, for  $q = 16–22$ , the (020) and (100) resonances have more or less substantial overlap with zero energy. The intensity rise in the threshold attachment mass spectrum (Fig. 1b) from  $q = 6$  to  $q = 5$  may be attributed to an influence of  $(\text{CO}_2)_N^-$  capture states without intramolecular excitation (but possibly some intermolecular excitation). One would expect such an influence to be even stronger for  $(\text{CO}_2)_4^-$  formation, but on the other hand the lifetimes of  $(\text{CO}_2)_N^-$  anions are expected to decrease at small  $N$ . With the sensitivity of our experiment,  $(\text{CO}_2)_4^-$  ions were the smallest anions observed.

## 4 Conclusions and outlook

Using a crossed beams apparatus a high resolution (energy width about 1 meV) laser photoelectron attachment study of negative ion formation involving CO<sub>2</sub> clusters has been carried out. Attachment spectra measured for  $(\text{CO}_2)_q^-$  ions ( $q = 4–22$ ) over the energy range 1–180 meV reveal that — similar to our previous findings for N<sub>2</sub>O aggregates — cluster ion formation is largely mediated through temporary negative ion states (vibrational Feshbach resonances VFRs) of the type  $[(\text{CO}_2)_{N-1}\text{CO}_2(\nu_i)]^-$  associated with intramolecular vibrational excitation. The “zero energy resonance”, observed some time ago at low electron energy resolution [17, 19], is thus explained by a superposition of several contributing VFRs which — when shifted to zero energy — enhance threshold electron attachment and thus produce and explain the strongly  $q$ -dependent threshold attachment mass spectrum. The widths and redshifts of the VFRs observed in  $(\text{CO}_2)_q^-$  formation are substantially larger than those found in negative ion formation from N<sub>2</sub>O clusters. Experiments on clusters of OCS and CS<sub>2</sub> are in progress. For CS<sub>2</sub> clusters no VFRs, but a strong increase of the attachment yield towards zero energy is observed. For OCS clusters preliminary results indicate the presence of VFRs.

This work was supported by the Deutsche Forschungsgemeinschaft (Schwerpunktprogramm *Molekulare Cluster* and Forschergruppe *Niederenergetische Elektronenstreuprozesse*), by the Graduiertenkolleg *Laser- und Teilchenspektroskopie* and through the Zentrum für Lasermeßtechnik und Diagnostik. We gratefully acknowledge L.S. Cederbaum for helpful discussions. IIF thanks the members of the Forschergruppe for their hospitality during his stay at Fachbereich Physik, Universität Kaiserslautern, and the US National Science Foundation for support through grant PHY-9801871.

## References

1. G.J. Schulz, *Rev. Mod. Phys.* **45**, 423 (1973).
2. R.N. Compton, in *Electronic and Atomic Collisions*, edited by N. Oda, K. Takayanagi (North-Holland, Amsterdam, 1980), p. 251.
3. *Electron-Molecule Interactions and their Applications*, edited by L.G. Christophorou (Academic Press, New York, 1984), Vols. 1 and 2.
4. M. Allan, *J. Electron Spectrosc.* **48**, 219 (1989).
5. T.D. Märk, *Int. J. Mass Spectrom. Ion Processes* **107**, 143 (1991).
6. E. Illenberger, *Chem. Rev.* **92**, 1589 (1992).
7. O. Ingólfsson, F. Weik, E. Illenberger, *Int. J. Mass Spectrom. Ion Proc.* **155**, 1 (1996).
8. W. Domcke, L.S. Cederbaum, *J. Phys. B* **14**, 149 (1981).
9. J. Gauyacq, A. Herzenberg, *Phys. Rev. A* **25**, 2959 (1982).
10. G. Knoth, M. Gote, M. Rädle, K. Jung, H. Ehrhardt, *Phys. Rev. Lett.* **62**, 1735 (1989).
11. A. Schramm, I.I. Fabrikant, J.M. Weber, E. Leber, M.-W. Ruf, H. Hotop, *J. Phys. B* **32**, 2153 (1999).
12. E. Leber, I.I. Fabrikant, J.M. Weber, M.-W. Ruf, H. Hotop, in *Dissociative Recombination: Theory, Experiment, and Applications IV*, edited by M. Larsson, J.B.A. Mitchell, I.F. Schneidev (World Scientific, Singapore, 2000), pp. 69-76; J.M. Weber, I.I. Fabrikant, E. Leber, M.-W. Ruf, H. Hotop, *Eur. Phys. J. D* **11**, 247 (2000).
13. J.M. Weber, E. Leber, M.-W. Ruf, H. Hotop, *Phys. Rev. Lett.* **82**, 516 (1999).
14. C.E. Klots, R.N. Compton, *J. Chem. Phys.* **69**, 1636 (1978).
15. M. Knapp, D. Kreisle, O. Echt, K. Sattler, E. Recknagel, *Surf. Sci.* **156**, 313 (1985).
16. M. Knapp, O. Echt, D. Kreisle, T.D. Märk, E. Recknagel, *Chem. Phys. Lett.* **126**, 225 (1986).
17. M. Knapp, O. Echt, D. Kreisle, T.D. Märk, E. Recknagel, in *Physics and Chemistry of Small Clusters*, edited by P. Jena, B.K. Rao, S.N. Kanna (Plenum Publ. Corp., 1987), p. 693.
18. A. Stamatovic, K. Stephan, T.D. Märk, *Int. J. Mass Spectrom. Ion Proc.* **63**, 37 (1985).
19. A. Stamatovic, K. Leiter, W. Ritter, K. Stephan, T.D. Märk, *J. Chem. Phys.* **83**, 2942 (1985).
20. D. Spence, G.J. Schulz, *Phys. Rev.* **188**, 280 (1969).
21. N.L. Alexander, M.A. Johnson, N.E. Levinger, W.C. Lineberger, *Phys. Rev. Lett.* **57**, 976 (1986).
22. H. Haberland, C. Ludewigt, H.-G. Schindler, D.R. Worsnop, in *Large Finite Systems*, edited by J. Jortner, A. Pullman, B. Pullman (D. Reidel Publ. Comp., 1987), p. 195.
23. T. Kondow, *J. Phys. Chem.* **91**, 1307 (1987).
24. F. Misaizu, K. Mitsuke, T. Kondow, K. Kuchitsu, *J. Chem. Phys.* **94**, 243 (1991).
25. T. Kraft, M.-W. Ruf, H. Hotop, *Z. Phys. D* **14**, 179 (1989).
26. M. Tsukada, N. Shima, S. Tsuneyuki, H. Kageshima, T. Kondow, *J. Chem. Phys.* **87**, 3927 (1987).
27. M.J. DeLuca, B. Niu, M.A. Johnson, *J. Chem. Phys.* **88**, 5857 (1988).
28. T. Tsukada, M. A. Johnson, T. Nagata, *Chem. Phys. Lett.* **268**, 429 (1997).
29. J.M. Weber, E. Leber, M.-W. Ruf, H. Hotop, *Eur. Phys. J. D* **7**, 587 (1999).
30. D. Klar, M.-W. Ruf, H. Hotop, *Chem. Phys. Lett.* **189**, 448 (1992); *Aust. J. Phys.* **45**, 263 (1992).
31. D. Klar, M.-W. Ruf, H. Hotop, *Meas. Sci. Technol.* **5**, 1248 (1994).
32. D. Klar, B. Mirbach, H.J. Korsch, M.-W. Ruf, H. Hotop, *Z. Phys. D* **31**, 235 (1994).
33. F.B. Dunning, *J. Phys. B* **28**, 1645 (1995).
34. *CRC Handbook of Chemistry and Physics*, edited by D.R. Lide, 76th edn. (Boca Raton, FL: Chemical Rubber Company, 1995).
35. M. Falk, *J. Chem. Phys.* **86**, 560 (1987).
36. A. Anderson, T. Sun, *Chem. Phys. Lett.* **8**, 537 (1971).
37. T.E. Gough, R.E. Miller, G. Scoles, *J. Phys. Chem.* **85**, 4041 (1981).
38. T.E. Gough, T.-Y. Wang, *Chem. Phys. Lett.* **207**, 517 (1993).
39. M.A. Ovchinnikov, C.A. Wight, *J. Chem. Phys.* **99**, 3374 (1993); *J. Chem. Phys.* **100**, 972 (1994).
40. F. Fleyfel, J.P. Devlin, *J. Phys. Chem.* **93**, 7292 (1989).
41. G. Herzberg, in *Molecular Spectra and Molecular Structure II: Infrared and Raman Spectra of Polyatomic Molecules* (van Nostrand Reinhold, N.Y., 1945).
42. P. Stampfli, *Phys. Rep.* **255**, 1 (1995).
43. J.J. Lowke, A.V. Phelps, B.W. Irwin, *J. Appl. Phys.* **44**, 4664 (1973).
44. M.A. Morrison, N.F. Lane, L.A. Collins, *Phys. Rev. A* **15**, 2186 (1977).
45. D. Field, S.L. Lunt, G. Mrotzek, J. Randell, J.P. Ziesel, *J. Phys. B* **24**, 3497 (1991).
46. C. Szmytkowski, A. Zecca, G. Karwasz, S. Oss, K. Maciag, B. Marinkovic, R.S. Brusa, R. Grisenti, *J. Phys. B* **20**, 5817 (1987).
47. F.A. Gianturco, T. Stoecklin, *J. Phys. B* **29**, 3933 (1996).
48. L.A. Morgan, *Phys. Rev. Lett.* **80**, 1873 (1998).
49. I.I. Fabrikant, *J. Phys. B* **17**, 4223 (1984).
50. P. Valiron, R. Gayet, R. McCarroll, F. Masnou-Seeuws, M. Philippe, *J. Phys. B* **12**, 53 (1979).
51. C. Szmytkowski, G. Karwasz, K. Maciag, *Chem. Phys. Lett.* **107**, 481 (1984).
52. B.K. Sarpal, K. Pfungst, B.M. Nestmann, S.D. Peyerimhoff, *J. Phys. B* **29**, 857 (1996); *ibid.* **29**, 1877 (1996).
53. C. Winstead, V. McKoy, *Phys. Rev. A* **57**, 3589 (1998).